Data report: radiography and X-ray CT imaging of whole core from IODP Expedition 308, Gulf of Mexico[1]

H.M. Nelson,[2] P.B. Flemings,[3] J.T. Germaine,[4] and B.E. Dugan[5]

Chapter contents

[1] Nelson, H.M., Flemings, P.B., Germaine, J.T., and Dugan, B.E., 2009. Data report: radiography and X-ray CT imaging of whole core from IODP Expedition 308, Gulf of Mexico. *In* Flemings, P.B., Behrmann, J.H., John, C.M., and the Expedition 308 Scientists, *Proc. IODP,* 308: College Station, TX (Integrated Ocean Drilling Program Management International, Inc.). doi:10.2204/iodp.proc.308.213.2009
[2] Department of Geosciences, The Pennsylvania State University, University Park PA 16802, USA. hnelson@geosc.psu.edu
[3] John A. and Katherine G. Jackson School of Geosciences, The University of Texas at Austin, Austin TX 78712, USA.
[4] Department of Civil and Environmental Engineering, Massachusetts Institute of Technology, Cambridge MA 02139, USA.
[5] Department of Earth Science, Rice University, Houston TX 77005, USA.

Abstract

We completed 151 radiographs and 12 X-ray computed tomography (CT) scans from whole cores taken during Integrated Ocean Drilling Program (IODP) Expedition 308. In Brazos-Trinity Basin IV, 29 radiographs and 1 X-ray CT scan were taken at Sites U1319 and U1320. In Ursa Basin, 122 radiographs and 11 X-ray CT scans were taken at Sites U1322 and U1324. These radiographs and X-ray CT scans were completed to select undisturbed portions of the core for experiments and to qualitatively assess the presence of inclusions and variation in the whole-core soil samples from the expedition. The imaging was performed at three locations: Pennsylvania State University, Massachusetts Institute of Technology, and Rice University.

Introduction

Integrated Ocean Drilling Program (IODP) Expedition 308 focused on how geology, pressure, and stress couple to control overpressure and fluid flow on the Gulf of Mexico continental slope (see the **"Expedition 308 summary"** chapter). To achieve this study, four sites were drilled and cored in two distinct areas in the Gulf of Mexico (Fig. **F1**). Two sites (U1319 and U1320) were drilled in a normally pressured area, Brazos-Trinity Basin IV (Fig. **F2**). The other two sites (U1322 and U1324) were drilled in an overpressured area, Ursa Basin (Fig. **F3**).

Whole-core geotechnical samples were taken at each of the four sites (U1319, U1320, U1322, and U1324) for the purpose of performing shore-based consolidation tests. To determine which soil samples to use for the experiments, noninvasive imaging was needed to evaluate the structure of the sample. This imaging was done using radiographs and X-ray computed tomography (CT) scans.

Most of the Pennsylvania State University (PSU) and Massachusetts Institute of Technology (MIT) samples were X-rayed at MIT's radiography facility. The Rice University samples were X-rayed by Fugro. The goal of imaging the soil was to qualitatively assess the presence of inclusions and variation in fabric, identify layering or inhomogeneities, and select undisturbed portions for experiments (**Long et al.**). Once the radiographs were completed they were shipped to PFS Photo in Christiansburg, Virginia, for digital

doi:10.2204/iodp.proc.308.213.2009

conversion. X-ray CT scans were performed by the Center for Quantitative Imaging (CQI) at PSU.

Tables T1 and T2 contain information on the 151 radiographs (Table T1) and 12 X-ray CT scans (Table T2) that were performed on the whole-core samples. These tables include sample identifiers such as, site, hole, core, and section. They also include the sample depth in meters below seafloor (mbsf) and the length of the sample in centimeters, including the top and bottom measurements. These data are used to pinpoint the exact location of the sample in the image with respect to the whole core. Samples were recovered by advanced piston corer (APC) or extended core barrel (XCB) technology. During APC, two different cutting shoes were used: the "Fugro" and "IODP-APC" cutting shoes. The Fugro cutting shoe has a thinner kerf than the IODP-APC cutting shoe and was used to try and reduce deformation during coring. Also listed in Tables T1 and T2 are the samples that were used for constant rate of strain consolidation (CRS) experiments (Long et al.). The individual digital images (.pdf format) can be found in "Supplementary material."

Methodology

Whole-core handling and preparation

During Expedition 308, the coring techniques included APC and XCB systems. These standard coring systems and their characteristics are summarized in *Technical Note* 31 of the Ocean Drilling Program (Graber et al., 2002). The sample was not extruded from the core liner on board the drilling ship. Whole-core samples were capped and sealed in wax to maintain natural saturation during refrigerated shipping and storage.

Radiography

Samples were X-rayed at MIT's radiography facility using a procedure similar to that described by American Society for Testing and Materials (ASTM) D4452 (ASTM International, 2003) in order to assess the sample quality, general material type, presence of inclusions, and variation in macrofabric (e.g., uniform, stratified, etc.). This information was used to help select the most appropriate and highest quality material for testing.

Figure F4 (Sauls, 1984) shows a schematic of the procedure for radiographing soil that is in 3 inch diameter steel tubes typically 2–3 ft long. Since the tubes are cylindrical, X-rays that strike the center of the tube (point A, Fig. F4) must travel through 0.2 inches of steel and 2.8 inches of soil, whereas those hitting point B penetrate much less soil. Therefore, aluminum plates of varying thickness are positioned in front of the specimen such that all X-rays will penetrate an approximately equal mass. Vertical lines in the photograph are caused by abrupt changes in the thickness at the edges of these aluminum plates and the black background results from lead shielding placed around the tube to reduce scattered radiation. Lead numbers and letters are attached at 1 inch intervals along the length of the tube to provide distance reference marks. At MIT, the tubes are radiographed in 10 inch segments to minimize the divergence of the X-ray beam. Each segment is exposed for about 5 min. The radiation is generated by a metal ceramic, double focus, beryllium X-ray tube that is excited by a Philips MG151-160 kV constant potential high-voltage generator. The radiographs are generated at full capacity of the system (160 kV and 3.8 mA).

The radiograph image is recorded on plate film. These negatives (much like those used in a doctor's office) are very difficult to work with in the laboratory. Therefore, the image is printed onto paper, yielding a photographic positive. On the positive print, dense objects appear white and voids appear black. The final product is slightly larger (~5%) than the actual size of the soil sample.

The image produced on the radiograph is an integration of all the material along the line from the radiograph source to the film. Changes in darkness depend on the relative absorption capacity of the materials being penetrated (i.e., steel, soil, air, shells, etc.). As a result, some features do not cause a sufficient change in absorption capacity and hence cannot be seen on the photograph. Other features are only visible when X-rays penetrate at the correct orientation. For example, an inclined crack filled with air within the sample will not be seen unless the X-ray path is parallel to the crack orientation. In general, changes in absorption capacity (absorption capacity is generally equated to density) as small as 5% can be observed.

Because of database issues and Fugro's methods of data archiving, we were unable to obtain specific information with regard to their equipment and methodology. For our qualitative study of the radiographs, this information would have been useful but is not critical for our research.

X-ray CT scans at PSU

X-ray CT imaging was performed by Abraham Grader at CQI. The machine used was a medical-based scanner, HD350. CQI used 130 kV and 100 mA energy settings and scanned all the cores at a resolution of ~0.2 mm × 0.2 mm × 0.2 mm. Volumetric imaging of the sample was completed by X-ray CT

(Universal Systems Inc.) as a sequence of stacked sections orthogonal to the long axis of the core (Yasuhara at al., 2006). Each CT slide image has two orthogonal longitudinal views through the center of the cores. The color scale is between 1000 (black) and 1500 (white).

Imaging results

Radiographs

Table T1 summarizes the details of each radiograph. A total of 122 radiographs from 65 samples were taken from Sites U1322 and U1324 in Ursa Basin. In Brazos-Trinity Basin IV, 29 radiographs were completed on 24 samples at Sites U1319 and U1320. Table T1 includes sample location information such as site, hole, and core number.

Each entry in Table T1 is associated with a digital image (.pdf format), which is provided in "Supplementary material." The images were created at one of two different locations: Fugro and the MIT radiography facility. Table T1 shows where each image was created. All of the Fugro images and 12 MIT images are shown as a positive print, where dense objects appear white and voids appear black. Figure F5 shows an example of this type of print at Site U1324. The remaining MIT images are shown as a negative print, where dense objects appear dark and voids appear white. Figure F6 shows an example of this type of print at Site U1324. The "inclusions" column in Table T1 summarizes the positive and negative print information.

X-ray CT scans

Table T2 summarizes the details of each X-ray CT scan. A total of 11 CT scans from 7 samples were taken from Sites U1322 and U1324 in Ursa Basin. In Brazos-Trinity Basin IV, one CT scan was completed on one sample at Site U1320. Table T2 includes sample location information such as site, hole, and core number.

Each entry in Table T2 is associated with a digital image (.pdf format), which is provided in "Supplementary material." The images were created at CQI. The X-ray CT scans are shown as a positive print, where dense objects appear white and voids appear black. Figure F7 shows an example of CT scans at Site U1324.

Also included in "Supplementary material" are four movies (.mpeg files) from Sample 308-U1324C-2H-4, 50–100 cm. The movies include: (A) a fly through on axial CT slices, (B) the sample rolling on its short axis, (C) the sample rolling on its longitudinal axis, and (D) a fly through on the samples longitudinal sections. These movies, which were created using X-ray CT scans, show a three-dimensional perspective of a sample that can not be seen with a radiograph.

Acknowledgments

This research used samples provided by the Integrated Ocean Drilling Program (IODP). Funding for this research was provided by the U.S. Science Support Program. In addition, U.S. National Science Foundation Grants 0447235 and 0351085 supported this research. This research was also sponsored by the Petroleum Research Fund (PRF# 44476-AC8). Thank you to Avrami Grader and the Center for Quantitative Imaging.

References

ASTM International, 2003. Standard test methods for X-ray radiography of soil samples (Standard D4452-85[2002]). In *Annual Book of ASTM Standards* (Vol. 04.08): *Soil and Rock* (I): West Conshohocken, PA (Am. Soc. Testing and Mater.), 686–699.

Graber, K.K., Pollard, E., Jonasson, B., and Schulte, E. (Eds.), 2002. Overview of Ocean Drilling Program engineering tools and hardware. *ODP Tech. Note,* 31. doi:10.2973/odp.tn.31.2002

Sauls, D.P., 1984. Strength-deformation properties of Harrison Bay arctic silts [M.S. thesis]. Massachusetts Institute of Technology, Boston.

Yasuhara, H., Polak, A., Mitani, Y., Grader, A.S., Halleck, P.M., and Elsworth D., 2006. Evolution of fracture permeability through fluid-rock reaction under hydrothermal conditions. *Earth Planet. Sci. Lett.,* 244(1–2):186–200. doi:10.1016/j.epsl.2006.01.046

Initial receipt: 7 July 2008
Acceptance: 6 October 2008
Publication: 31 March 2009
MS 308-213

Figure F1. Basemap of the study areas on the continental shelf, Gulf of Mexico. Brazos-Trinity Basin IV is 200 km due south of Galveston, Texas, USA, in ~1400 m of water. Ursa Basin is ~200 km southeast of Louisiana, USA, in ~1000 m of water. NGDC = National Geophysical Data Center, NOAA = National Oceanic and Atmospheric Administration.

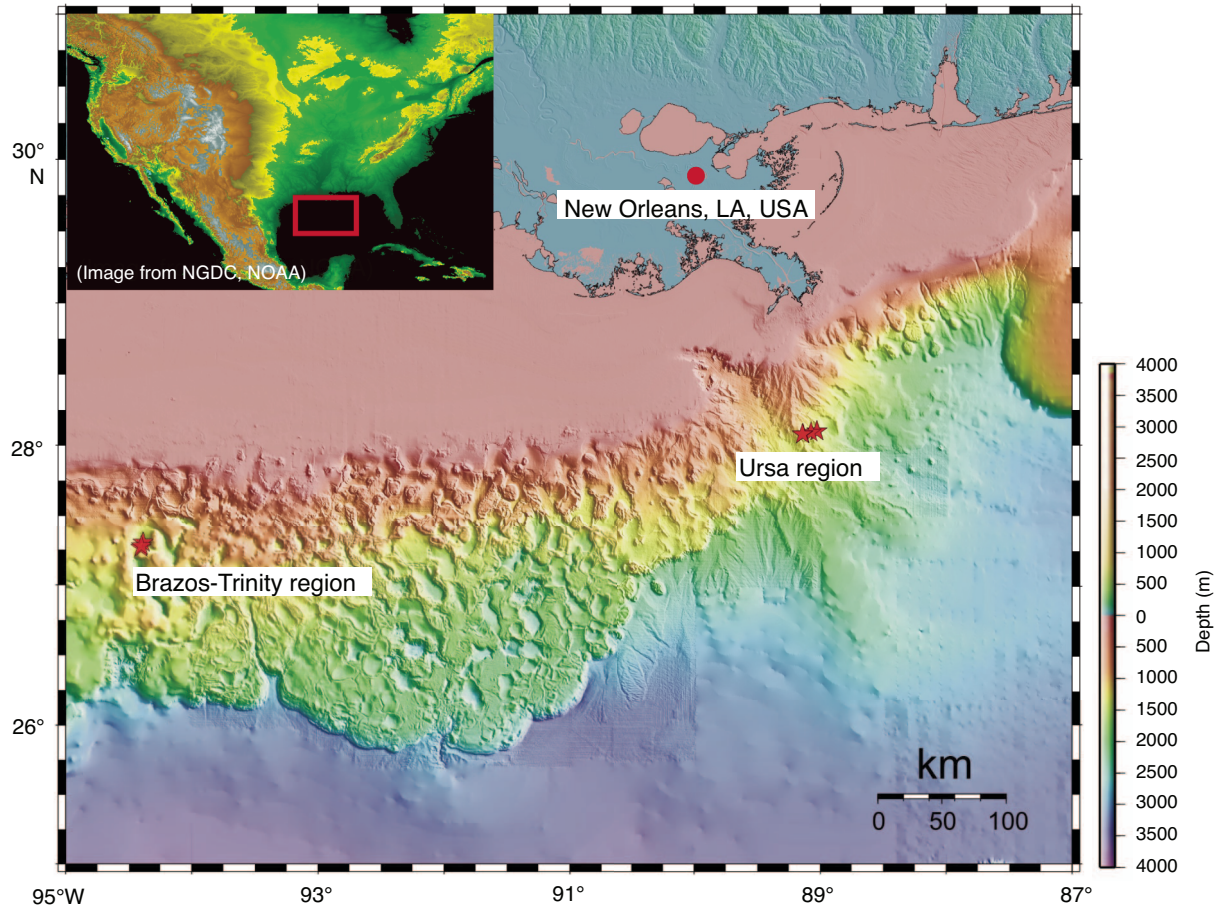

Figure F2. Seismic cross section of Brazos-Trinity Basin IV, Sites U1319 and U1320. SF = seafloor.

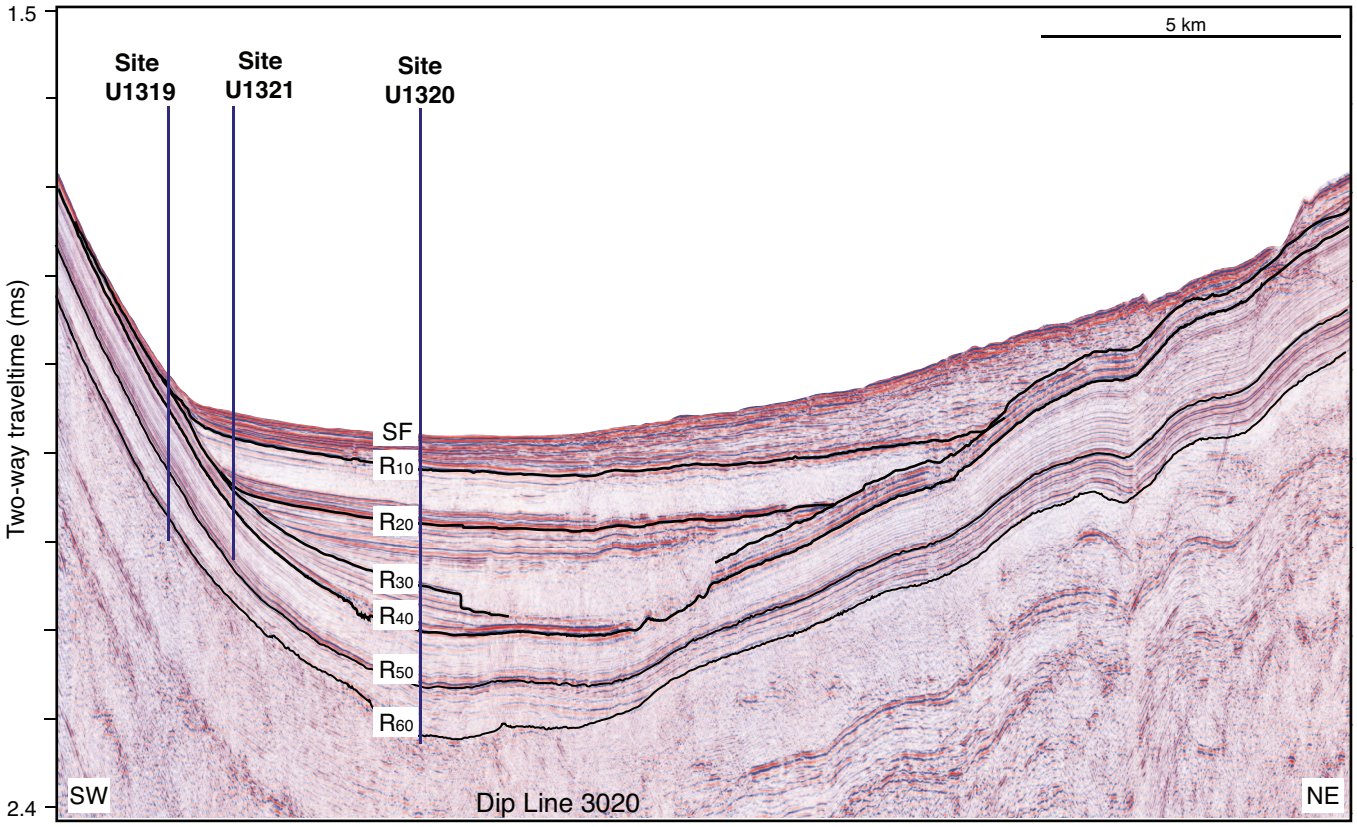

Figure F3. A. Seismic cross section of Ursa Basin, Sites U1322 and U1324. **B.** Interpreted cross section. MTD = mass transport deposit.

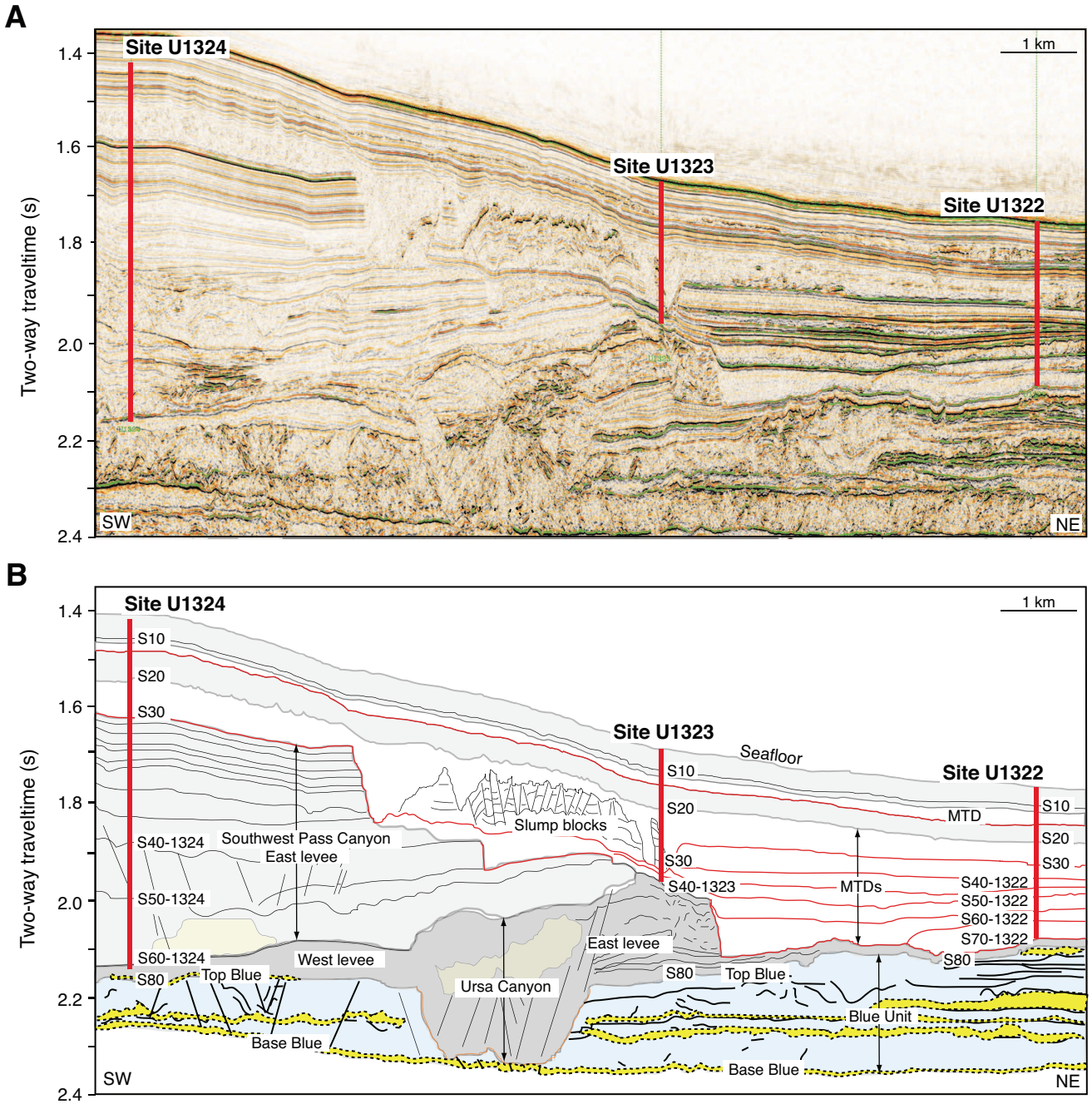

Figure F4. Schematic diagram of the method used to X-ray whole-core soil samples at MIT (Sauls, 1984). **A.** Elevation view. **B.** Side view.

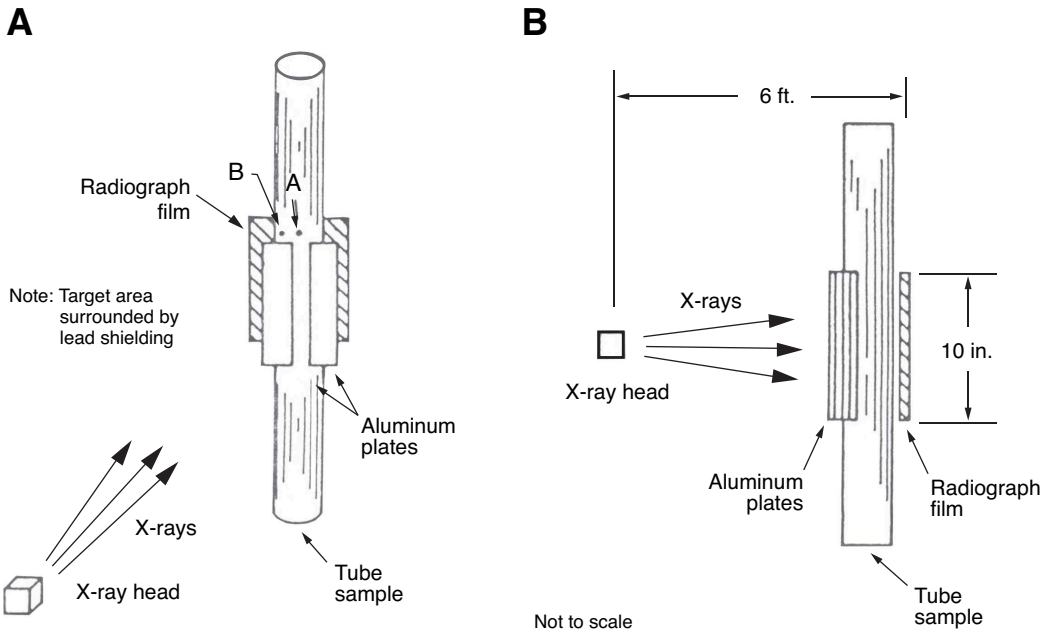

Figure F5. Positive radiograph (see Table T1) from Ursa Basin, Site U1324 (Sample 308-U1324C-5H-3, 90–115 cm). Radiograph was completed by Fugro for Rice University. Dark colors = low densities and are interpreted as voids, light colors = higher densities typical of sediment.

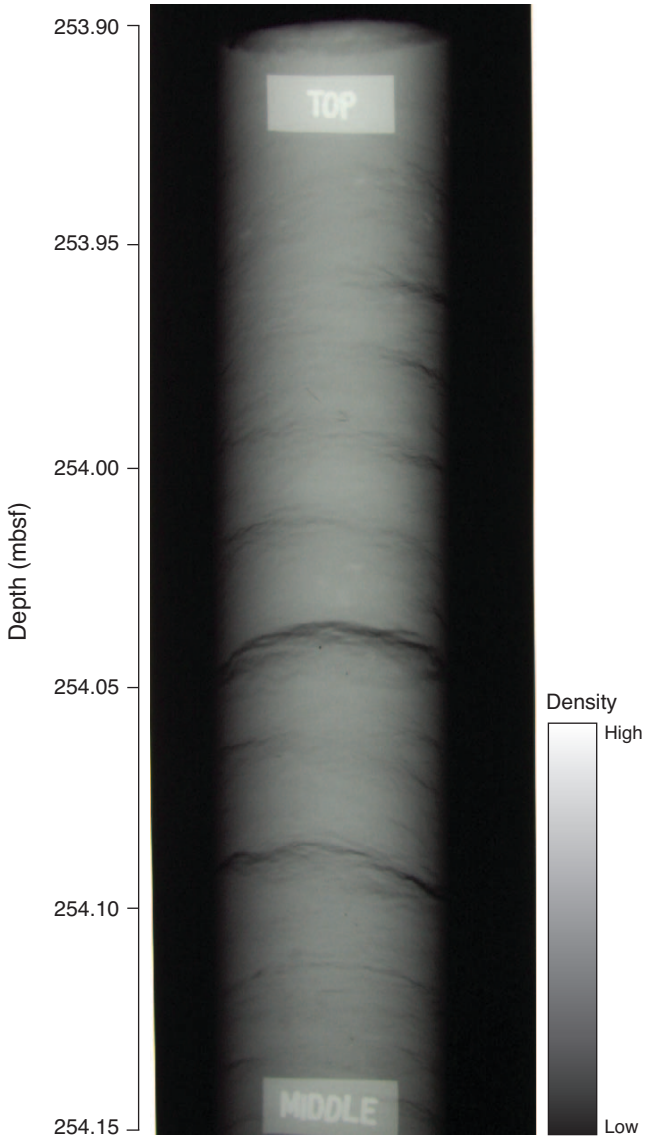

Figure F6. Negative radiograph (see Table T1) from Ursa Basin, Site U1324 (Sample 308-U1324C-8H-4, 75–100 cm). Radiograph was completed by MIT. Light colors = low densities and are interpreted as voids, dark colors = higher densities typical of sediment.

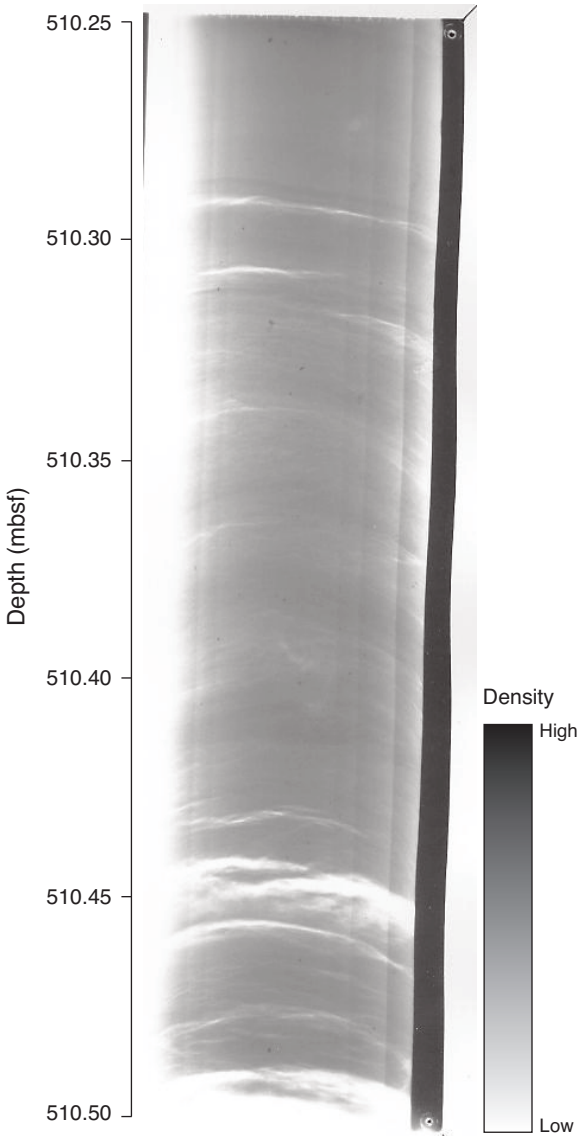

Figure F7. Positive X-ray CT scan from Ursa Basin, Site U1324 (Sample 308-U1324C-4H-4, 50–100 cm). CT image was completed by CQI. Dark colors = low densities and are interpreted as voids, light colors = higher densities typical of sediment.

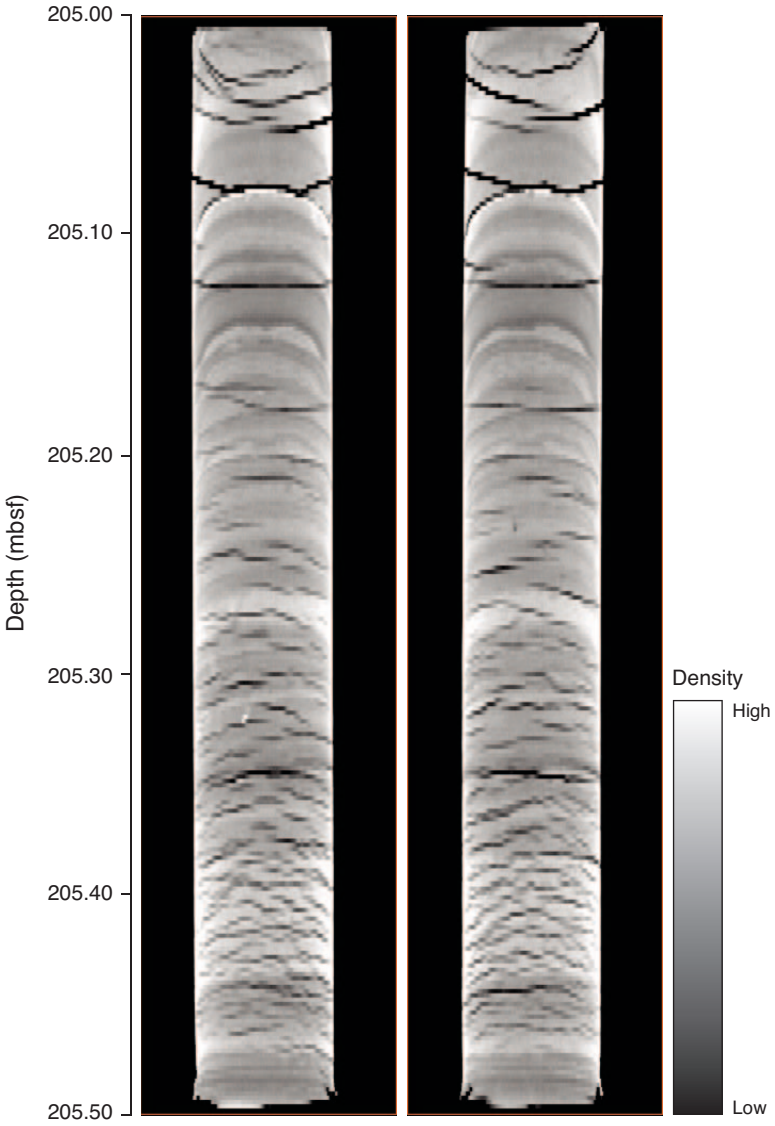

Table T1. Digital radiographs, Brazos-Trinity Basin IV and Ursa Basin. (See table notes.) (Continued on next two pages.)

Core, section, interval (cm)	Cutting shoe	Length of sample (cm)	Top of core depth (mbsf)	X-ray depth (mbsf) Top	X-ray depth (mbsf) Bottom	Scanning location	Pos/neg	Notes
308-U1319A-								
4H-4, 117–137	IODP-APC	20	28.00	29.17	29.37	Fugro	Positive	
6H-7, 58–78	IODP-APC	20	51.50	52.08	52.28	MIT	Positive	
7H-CC, 7–22	IODP-APC	15	61.85	61.92	62.07	MIT	Negative	
9H-6, 114–134	IODP-APC	20	78.50	79.64	79.84	Fugro	Positive	
9H-7, 0–25	IODP-APC	25	78.50	78.50	78.75	MIT	Positive	
9H-7, 25–50	IODP-APC	25	78.50	78.75	79.00	MIT	Positive	
9H-CC, 0–20	IODP-APC	20	80.40	80.40	80.60	MIT	Negative	
10H-CC, 0–18	IODP-APC	18	89.27	89.27	89.45	MIT	Negative	
10H-CC, 18–33	IODP-APC	15	89.27	89.45	89.60	MIT	Negative	
11H-8, 76–98	IODP-APC	22	98.62	99.38	99.60	MIT	Negative	
11H-CC, 0–19	IODP-APC	19	99.60	99.60	99.79	MIT	Negative	
12H-CC, 4–21	IODP-APC	17	106.23	106.27	106.44	MIT	Positive	
14X-4, 81–101	Fugro	20	118.60	119.41	119.61	MIT	Positive	
15X-1, 130–150	Fugro	20	119.10	120.40	120.60	Fugro	Positive	
15X-CC, 0–24	Fugro	24	126.09	126.09	126.33	MIT	Negative	
308-U1320A-								
4H-7, 25–45	IODP-APC	20	32.35	32.60	32.80	Fugro	Positive	
12X-3, 92–112	Fugro	20	90.90	91.82	92.02	Fugro	Positive	
16X-1, 130–150	Fugro	20	126.30	127.60	127.80	Fugro	Positive	
23X-6, 93–113	Fugro	20	201.30	202.23	202.43	MIT	Negative	
23X-7, 0–25	Fugro	25	202.43	202.43	202.68	MIT	Negative	
23X-7, 25–51	Fugro	26	202.43	202.68	202.94	MIT	Negative	
24X-6, 96–121	Fugro	25	210.90	211.85	212.11	MIT	Negative	
24X-6, 121–146	Fugro	25	210.90	212.11	212.36	MIT	Negative	
26X-3, 112–132	Fugro	20	225.41	226.53	226.73	Fugro	Positive	
26X-CC, 0–25	Fugro	25	232.03	232.03	232.28	MIT	Negative	
27X-7, 0–23	Fugro	23	241.20	241.20	241.43	MIT	Negative	
31X-3, 120–140	Fugro	20	273.70	274.90	275.10	Fugro	Positive	
32X-6, 0–25	Fugro	25	287.30	287.30	287.55	MIT	Negative	
32X-6, 25–50	Fugro	25	287.30	287.55	287.80	MIT	Negative	
308-U1322B-								
4H-3, 117–137	Fugro	20	26.00	27.17	27.37	Fugro	Positive	CRS Test 815
9H-5, 130–150	IODP-APC	20	76.50	77.80	78.00	Fugro	Positive	
13H-6, 40–60	IODP-APC	20	114.56	114.96	115.16	MIT	Negative	
15H-1, 100–111	IODP-APC	11	124.80	125.80	125.91	MIT	Positive	CRS Test 808
16H-1, 130–150	Fugro	20	134.30	135.60	135.80	Fugro	Positive	
18H-6, 0–25	Fugro	25	156.90	156.90	157.15	MIT	Positive	
18H-6, 25–40	Fugro	15	156.90	157.16	157.30	MIT	Positive	CRS Test 810
21H-3, 112–132	IODP-APC	20	177.50	178.62	178.82	Fugro	Positive	CRS Test 825
26H-1, 102–122	Fugro	20	210.30	211.32	211.52	Fugro	Positive	
29H-1, 100–125	IODP-APC	25	227.10	228.10	228.35	MIT	Negative	
29H-1, 125–150	IODP-APC	25	227.10	228.35	228.60	MIT	Negative	
308-U1322D-								
1H-2, 100–125	Fugro	25	41.50	42.50	42.75	MIT	Negative	
1H-2, 125–150	Fugro	25	41.50	42.75	43.00	MIT	Negative	CRS Test 826
1H-3, 40–65	Fugro	25	43.00	43.40	43.65	Fugro	Positive	
1H-3, 65–90	Fugro	25	43.00	43.65	43.90	Fugro	Positive	
1H-3, 90–115	Fugro	25	43.00	43.90	44.15	Fugro	Positive	
1H-3, 115–140	Fugro	25	43.00	44.15	44.40	Fugro	Positive	
1H-4, 50–75	Fugro	25	44.50	45.00	45.25	MIT	Negative	
1H-4, 75–100	Fugro	25	44.50	45.25	45.50	MIT	Negative	
2H-2, 100–125	Fugro	25	71.50	72.50	72.75	MIT	Negative	
2H-2, 125–150	Fugro	25	71.50	72.75	73.00	MIT	Negative	CRS Tests 796 and 798
2H-3, 40–65	Fugro	25	73.00	73.40	73.65	Fugro	Positive	
2H-3, 65–90	Fugro	25	73.00	73.65	73.90	Fugro	Positive	
2H-3, 90–115	Fugro	25	73.00	73.90	74.15	Fugro	Positive	
2H-3, 115–140	Fugro	25	73.00	74.15	74.40	Fugro	Positive	
2H-4, 50–75	Fugro	25	74.50	75.00	75.25	MIT	Negative	
2H-4, 75–100	Fugro	25	74.50	75.25	75.50	MIT	Negative	
3H-3, 40–65	Fugro	25	103.00	103.40	103.65	Fugro	Positive	CRS Test 021
3H-3, 65–90	Fugro	25	103.00	103.65	103.90	Fugro	Positive	
3H-3, 90–115	Fugro	25	103.00	103.90	104.15	Fugro	Positive	
3H-3, 115–140	Fugro	25	103.00	104.15	104.40	Fugro	Positive	

Table T1 (continued). (Continued on next page.)

Core, section, interval (cm)	Cutting shoe	Length of sample (cm)	Top of core depth (mbsf)	X-ray depth (mbsf) Top	X-ray depth (mbsf) Bottom	Scanning location	Pos/neg	Notes
308-U1324B-								
3H-CC, 0–24	IODP-APC	24	22.89	22.89	23.13	MIT	Positive	
4H-1, 125–145	Fugro	20	22.80	24.05	24.25	Fugro	Positive	
4H-3, 117–137	Fugro	20	25.80	26.97	27.17	Fugro	Positive	
4H-7, 56–116	Fugro	60	31.30	31.86	32.46	Fugro	Positive	CRS Tests 013, 014, and 800
5H-7, 0–53	IODP-APC	53	41.30	41.30	41.83	Fugro	Positive	
7H-7, 0–63	Fugro	63	60.31	60.31	60.94	Fugro	Positive	CRS Tests 015 and 802
8H-CC,0–25	IODP-APC	25	70.33	70.33	70.58	MIT	Positive	
9H-5, 120–140	IODP-APC	20	76.30	77.50	77.70	Fugro	Positive	
10H-7, 0–25	IODP-APC	25	88.80	88.80	89.05	MIT	Positive	
10H-7, 25–45	IODP-APC	20	88.80	89.05	89.25	MIT	Negative	CRS Test 813
13H-7, 15–35	Fugro	20	117.09	117.24	117.44	MIT	Negative	CRS Test 05
13H-7, 35–60	Fugro	25	117.09	117.44	117.69	MIT	Negative	
13H-7, 60–85	Fugro	25	117.09	117.69	117.94	MIT	Negative	
15H-5, 90–150	IODP-APC	60	133.30	134.20	134.80	Fugro	Positive	CRS Test 803
16H-1, 130–150	IODP-APC	20	136.30	137.60	137.80	Fugro	Positive	
16H-5, 90–150	IODP-APC	60	141.23	142.13	142.73	Fugro	Positive	CRS Test 801
18H-6, 29–49	IODP-APC	20	161.20	161.49	161.69	MIT	Negative	
20H-6, 0–25	IODP-APC	25	178.18	178.18	178.43	MIT	Negative	
20H-6, 25–51	IODP-APC	26	178.18	178.43	178.69	MIT	Negative	
21H-3, 112–132	Fugro	20	182.00	183.12	183.32	Fugro	Positive	CRS Test 020
23H-5, 0–22	Fugro	22	199.80	199.80	200.02	MIT	Positive	CRS Test 812
26H-3, 122–142	IODP-APC	20	219.10	220.32	220.52	Fugro	Positive	CRS Test 018
27H-5, 25–50	Fugro	25	228.00	228.25	228.50	MIT	Negative	
27H-5, 50–75	Fugro	25	228.00	228.50	228.75	MIT	Negative	
28H-7, 43–63	IODP-APC	20	237.62	238.05	238.25	MIT	Negative	
31H-3, 120–140	Fugro	20	259.80	261.00	261.20	Fugro	Positive	CRS Test 019
37H-3, 120–140	Fugro	20	308.60	309.80	310.00	Fugro	Positive	
42H-1, 130–150	IODP-APC	20	339.00	340.30	340.50	Fugro	Positive	
44H-1, 120–140	IODP-APC	20	352.70	353.90	354.10	MIT	Negative	
48H-2, 130–150	IODP-APC	20	374.70	376.00	376.20	Fugro	Positive	
53X-4, 130–150	Fugro	20	410.90	412.20	412.40	Fugro	Positive	
58X-4, 130–150	Fugro	20	459.10	460.40	460.60	Fugro	Positive	
69X-2, 120–140	Fugro	20	561.90	563.10	563.30	Fugro	Positive	
308-U1324C-								
1H-2, 70–95	IODP-APC	25	51.50	52.20	52.45	MIT	Negative	CQI scanned
1H-2, 95–120	IODP-APC	25	51.50	52.45	52.70	MIT	Negative	CQI scanned
1H-3, 30–55	IODP-APC	25	53.00	53.30	53.55	Fugro	Positive	
1H-3, 55–80	IODP-APC	25	53.00	53.55	53.80	Fugro	Positive	
1H-3, 80–105	IODP-APC	25	53.00	53.80	54.05	Fugro	Positive	
1H-3, 105–130	IODP-APC	25	53.00	54.05	54.30	Fugro	Positive	
1H-4, 130–150	IODP-APC	20	54.50	55.80	56.00	MIT	Negative	
1H-5, 115–130	IODP-APC	15	56.00	57.15	57.30	MIT	Negative	
1H-6, 135–150	IODP-APC	15	57.50	58.85	59.00	MIT	Negative	
1H-7, 18–33	IODP-APC	15	59.00	59.18	59.33	MIT	Negative	
2H-3, 40–65	Fugro	25	103.00	103.40	103.65	Fugro	Positive	
2H-3, 65–90	Fugro	25	103.00	103.65	103.90	Fugro	Positive	
2H-3, 90–115	Fugro	25	103.00	103.90	104.15	Fugro	Positive	
2H-3, 115–140	Fugro	25	103.00	104.15	104.40	Fugro	Positive	
2H-4, 52–75	Fugro	25	104.50	105.02	105.25	MIT	Negative	CQI scanned
2H-4, 75–100	Fugro	25	104.50	105.25	105.50	MIT	Negative	CQI scanned, CRS Test 807
3H-2, 50–75	IODP-APC	25	150.59	151.09	151.34	MIT	Negative	
3H-2, 75–100	IODP-APC	25	150.59	151.34	151.59	MIT	Negative	
3H-2, 100–125	IODP-APC	25	150.59	151.59	151.84	MIT	Negative	
3H-2, 125–150	IODP-APC	25	150.59	151.84	152.09	MIT	Negative	
3H-3, 40–65	IODP-APC	25	152.09	152.49	152.74	Fugro	Positive	
3H-3, 65–90	IODP-APC	25	152.09	152.74	152.99	Fugro	Positive	
3H-3, 90–115	IODP-APC	25	152.09	152.99	153.24	Fugro	Positive	
3H-3, 115–140	IODP-APC	25	152.09	153.24	153.49	Fugro	Positive	
3H-4, 50–75	IODP-APC	25	153.59	154.09	154.34	MIT	Negative	CQI scanned
3H-4, 75–100	IODP-APC	25	153.59	154.34	154.59	MIT	Negative	CQI scanned
4H-2, 50–75	Fugro	25	201.50	202.00	202.25	MIT	Negative	
4H-2, 75–100	Fugro	25	201.50	202.25	202.50	MIT	Negative	
4H-3, 40–65	Fugro	25	203.00	203.40	203.65	Fugro	Positive	
4H-3, 65–90	Fugro	25	203.00	203.65	203.90	Fugro	Positive	
4H-3, 90–115	Fugro	25	203.00	203.90	204.15	Fugro	Positive	
4H-3, 115–140	Fugro	25	203.00	204.15	204.40	Fugro	Positive	
4H-4, 50–75	Fugro	25	204.50	205.00	205.25	MIT	Negative	CQI scanned

Table T1 (continued).

Core, section, interval (cm)	Cutting shoe	Length of sample (cm)	Top of core depth (mbsf)	X-ray depth (mbsf) Top	X-ray depth (mbsf) Bottom	Scanning location	Pos/neg	Notes
4H-4, 75–100	Fugro	25	204.50	205.25	205.50	MIT	Negative	CQI scanned
4H-5, 18–43	Fugro	25	205.50	205.68	205.93	MIT	Negative	
4H-5, 43–68	Fugro	25	205.50	205.93	206.18	MIT	Negative	
5H-3, 40–65	IODP-APC	25	253.00	253.40	253.65	Fugro	Positive	
5H-3, 65–90	IODP-APC	25	253.00	253.65	253.90	Fugro	Positive	
5H-3, 90–115	IODP-APC	25	253.00	253.90	254.15	Fugro	Positive	
5H-3, 115–140	IODP-APC	25	253.00	254.15	254.40	Fugro	Positive	
6H-2, 40–65	Fugro	25	301.50	301.90	302.15	Fugro	Positive	
6H-2, 65–90	Fugro	25	301.50	302.15	302.40	Fugro	Positive	
6H-2, 90–115	Fugro	25	301.50	302.40	302.65	Fugro	Positive	
6H-2, 115–140	Fugro	25	301.50	302.65	302.90	Fugro	Positive	
6H-3, 0–25	Fugro	25	303.00	303.00	303.25	MIT	Negative	
6H-3, 25–50	Fugro	25	303.00	303.25	303.50	MIT	Negative	
6H-3, 50–75	Fugro	25	303.00	303.50	303.75	MIT	Negative	
6H-3, 75–106	Fugro	31	303.00	303.75	304.06	MIT	Negative	CRS Tests 001 and 002
7H-2, 40–65	IODP-APC	25	406.50	406.90	407.15	Fugro	Positive	
7H-2, 65–90	IODP-APC	25	406.50	407.15	407.40	Fugro	Positive	
7H-2, 90–115	IODP-APC	25	406.50	407.40	407.65	Fugro	Positive	
7H-2, 115–140	IODP-APC	25	406.50	407.65	407.90	Fugro	Positive	
8H-3, 40–65	Fugro	25	508.00	508.40	508.65	Fugro	Positive	
8H-3, 65–90	Fugro	25	508.00	508.65	508.90	Fugro	Positive	
8H-3, 90–115	Fugro	25	508.00	508.90	509.15	Fugro	Positive	
8H-3, 115–140	Fugro	25	508.00	509.15	509.40	Fugro	Positive	
8H-4, 50–75	Fugro	25	509.50	510.00	510.25	MIT	Negative	
8H-4, 75–100	Fugro	25	509.50	510.25	510.50	MIT	Negative	

Notes: APC = advanced piston corer. CRS = constant rate of strain experiments (see **Long et al.**), CQI = Center for Quantitative Imaging (see Table **T2**).

Table T2. X-ray CT images, Brazos-Trinity Basin IV and Ursa Basin. (**See table notes.**)

Core, section, interval (cm)	Cutting shoe	Length of sample (cm)	Top of core depth (mbsf)	CT scan depth (mbsf) Top	CT scan depth (mbsf) Bottom	Notes/CRS test
308-U1320A-						
19X-CC, 0–47	Fugro	47	164.54	164.54	165.01	CQI scan
308-U1324B-						
6H-7, 0–62	IODP-APC	62	50.80	50.80	51.42	CQI scan
60X-2, 130–150	Fugro	20	475.40	476.70	476.90	CQI scan
70X-6, 40–90	Fugro	50	577.27	577.67	578.17	CQI scan
308-U1324C-						
1H-2, 20–70	IODP-APC	50	51.50	51.70	52.20	CQI scan
1H-2, 70–120	IODP-APC	50	51.50	52.20	52.70	CQI scan
2H-4, 0–50	Fugro	50	104.50	104.50	105.00	CQI scan
2H-4, 50–100	Fugro	50	104.50	105.00	105.50	CQI scan, CRS Test 807, movies
3H-4, 0–50	IODP-APC	50	153.59	153.59	154.09	CQI scan
3H-4, 50–100	IODP-APC	50	153.59	154.09	154.59	CQI scan
4H-4, 0–50	Fugro	50	204.50	204.50	205.00	CQI scan
4H-4, 50–100	Fugro	50	204.50	205.00	205.50	CQI scan

Notes: APC = advanced piston corer. CT = computed tomography. CRS = constant rate of strain experiments (see **Long et al.**), CQI = Center for Quantitative Imaging, movies = digital movies available (see **"Supplementary material"**).